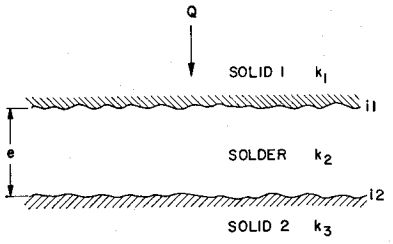

Fig. 1 Soldered joints.

two interfaces $i1$ and $i2$. The surfaces of two solids are nominally flat but rough and the thickness of the solder is much larger than the surface roughness.

The temperature fields far from the interfaces are unidirectional, parallel to the planes of the interfaces. In the vicinities of the interfaces and within the solder the temperature field is no longer unidirectional because of the waviness of the interfaces and the discontinuity of the thermal conductivity across the interfaces. The net result of this nonuniformity of temperature field is a measurable temperature drop ΔT_j at the joint. The thermal resistance at the joint is defined as $R_j = \Delta T_j/(Q/A)$ and can be written as $R_j = R_{i1} + R_{i2}$ where R_{i1} and R_{i2} are the interface resistances.

The thermal resistance at interface $i1$ is $R_{i1} = \psi_{i1}/k_{i1}$, where $k_{i1} = 2k_1k_2/(k_1 + k_2)$. The parameter ψ_{i1}, based upon current thermal constriction theory,[2-4] has the dimension cm and consists of a dimensionless geometric parameter and some characteristic dimension of the interface such as the surface roughness and the number of elemental heat flow channels available for heat conduction across the interface. The parameter ψ is assumed to be independent of thermal properties of the joint as well as the local heat flux. It will depend upon the surface roughness. The thermal resistance at the other interface can similarly be written as $R_{i2} = \psi_{i2}/k_{i2}$ where $k_{i2} = 2k_2k_3/(k_2 + k_3)$.

The total or joint resistance being the sum of the two interface resistances can be written as $R_j = \psi_{i1}/k_{i1} + \psi_{i2}/k_{i2}$. For identical surface conditions $\psi_{i1} = \psi_{i2}$ and so the joint resistance reduces to $R_j = \psi_i/K_j$ where $K_j = 2/(1/k_1 + 2/k_2 + 1/k_3)$. Here K_j is the effective thermal conductivity of a soldered joint consisting of three different materials having thermal conductivities k_1, k_2 and k_3, respectively.

Experimental Verification of the Theory

A series of tests was performed to verify the results of the thermal analysis. These tests consisted of temperature measurements in brass (k_1 = 1.11 w/cm-°C) and stainless steel (k_3 = 0.162 w/cm-°C) soldered with pure tin (k_2 = 0.64 w/cm-°C). The procedure followed is fully described in Ref. 1.

The first tests using brass/brass joints (K = 0.405 w/cm-°C) yielded a minimum resistance of 0.0245°C-cm²/w. The brass/stainless steel joints (K = 0.198 w/cm-°C) yielded a minimum resistance of 0.052°C-cm²/w and the stainless/stainless steel joints (K = 0.131 w/cm-°C) yielded a minimum resistance of 0.0805°C-cm²/w.

From these series of tests the parameter $\psi_i = [\Delta T_j/(Q/A)]K_j$ is calculated to have the values 0.0099, 0.0103, and 0.0109 for the three types of joints investigated. These values of ψ_i represent the average for ten sets of measurements obtained for each of the brass/brass, brass/stainless, and stainless/stainless joints. There was no observable variation of joint resistance with contact pressure.

Conclusions

The excellent agreement between the values of ψ_i obtained for the three types of soldered joints is a verification of the validity of the assumptions used. In these experiments the thermal conductivities differed by a factor of seven while the values of the effective thermal conductivity of the joints differed by a factor of three. One can conclude that the thermal resistance of a soldered joint can be correlated by means of the parameter ψ_i provided that the solder is homogeneous devoid of cavities and scale, and that ψ_i = 0.010 when the surface roughness is about 0.3 μ.

References

[1] Yovanovich, M. M. and Tuarze, M., "Experimental Evidence of Thermal Resistance at Soldered Joints," *Journal of Spacecraft and Rockets*, Vol. 6, No. 7, July 1969, pp. 855–857.

[2] Yovanovich, M. M., "Overall Constriction Resistance Between Contacting Rough, Wavy Surfaces," *International Journal of Heat and Mass Transfer*, Vol. 12, 1969, pp. 1517–1520.

[3] Mikic, B. B., "On Mechanism of Dropwise Condensation," *International Journal of Heat and Mass Transfer*, Vol. 12, 1969, pp. 1311–1324.

[4] Cooper, M. G., Mikic, B. B., and Yovanovich, M. M., "Thermal Contact Conductance," *International Journal of Heat and Mass Transfer*, Vol. 12, 1969, pp. 279–300.

Incipient Cross-Stream Liquid Jet Atomization at High Altitude and Velocity

PAUL B. GOODERUM* AND DENNIS M. BUSHNELL†
NASA Langley Research Center, Hampton, Va.

Nomenclature

D_o = orifice diameter
Kn = Knudsen number, $M(\gamma\pi/2)^{1/2}/Re$
M = Mach number, $(Vg^2 + V_l^2)^{1/2}/a$
Re = Reynolds number, $\rho(Vg^2 + V_l^2)^{1/2}D_o/\mu$
Vg = gas velocity
V_l = liquid velocity at the orifice
We = Weber number, $\rho(Vg^2 + V_l^2)D_o/2\sigma$
μ = coefficient of viscosity
ρ = density, gas stream
σ = surface tension, liquid

A FLIGHT research project has been conducted to measure the effects of a liquid spray on the electron and ion concentrations in the flow field over the antenna of a reentering vehicle.[1] In the analysis of these results it is of fundamental importance to know whether or not the liquid jets were broken up into the required spray.[2] Secondly, if breakup did occur, subsequent analyses of the flight data require knowledge of which of the basic breakup mechanisms (aerodynamic, vapor pressure, or capillary instability) was the dominant cause. The present investigation originated because of this need to define the boundaries of aerodynamic breakup.

An unbroken liquid stream exiting an orifice into a gaseous cross flow will be atomized if the cross-flow dynamic pressure is greater than a certain critical value[3,4] (assuming that the ambient pressure is such that vapor pressure or "flashing" breakup effects can be ignored). At dynamic pressures below this critical value, capillary instabilities[5] cause the jet to separate into drops which are then swept downstream with no further shatter. For purely aerodynamic breakup, there is ample theoretical and experimental evidence, mostly for drops, to indicate that the Weber number, which is the ratio of the dynamic pressure of the gas to the surface tension of the liquid, is useful as a correlating parameter.[6] However, before applying the available critical Weber number information to high altitude flight conditions, it is necessary to assess the applicability of data obtained at low speed, low Knudsen

Received March 6, 1970; revision received May 7, 1970.

*Aerospace Engineer, Aero-Physics Division. Member AIAA.

† Head, Flow Analysis Section, Aero-Physics Division.

number conditions, to the high Knudsen number conditions of flight (low density, high static temperature).

A summary of the available experimental data, restricted to liquid jets in 90° cross flows, low Weber number, ($We <$ 200), low viscosity (Ohnesorge numbers $\ll 1.0$), and with no vapor pressure effects,[7] is presented in Table 1a.[2-4,8-14] Only the lowest Weber number data were taken from any given source. In an attempt to determine the variation of critical Weber number with Knudsen number, the data of Table 1a were plotted in Fig. 1 as circles. It appears, from the resulting plot, that the no-breakup data point[3] represented by the closed circle (3) (at $Kn = 1.22 \times 10^{-4}$, $We = 21.9$) might be of doubtful accuracy as there are several breakup data points at lower Weber numbers but at approximately the same Knudsen number.

For comparison with the plotted experimental values, theoretical values for critical Weber number are available from several sources where theoretical We_{crit} at low Knudsen number for liquid jets[15] and drops[16] have been determined using simple analysis. The theory for droplet breakup is shown, even though the experimental data is for jet breakup, since the droplet breakup criterion is available for drops at low Reynolds numbers ($Re = 10$) and might be applicable at high Knudsen numbers. Available information indicates that jets and drops in continuum flow have similar We_{crit} values.[15] So, if we envision the theoretical boundary between stable and unstable-sized water drops as a line connecting the vertical dashed lines plotted at the top and bottom edge of the figure, then we might conclude that, at least to the extent that there are no breakup data to the left of our imaginary dotted line, there is good agreement between theory and experiment for liquid jet breakup in the continuum flow regime.

The flight vehicle flowfield values for Kn and We calculated for the injection site of a typical blunt reentry body[17] are also given in Table 1c and shown on Fig. 1. Streamline 2 represents flow-field conditions close to the body and streamline 8 the conditions immediately behind the shock wave at this body station.

To provide more confidence in the use of a critical We number atomization criterion at high Kn, it was decided to obtain some experimental data in this region. To simulate experimentally a water jet at its critical condition on a vehicle reentering the earth's atmosphere over an altitude range of

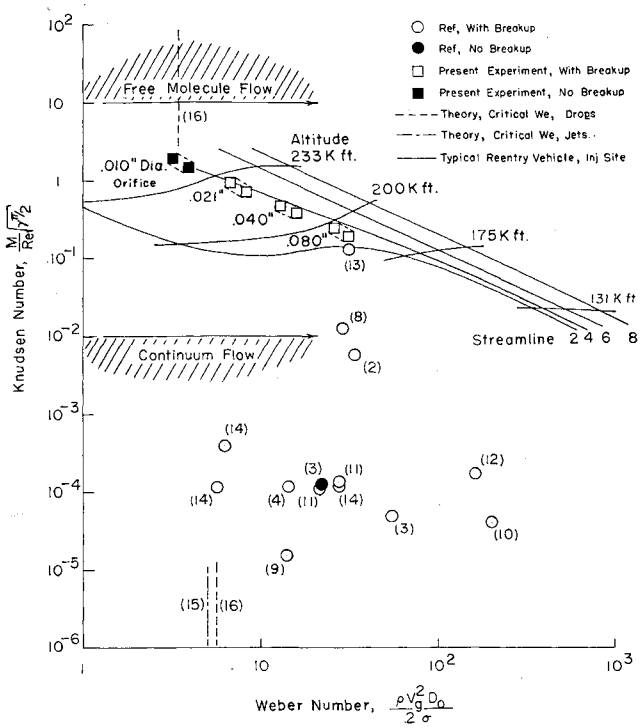

Fig. 1 Variation of Weber number with Knudsen number for various liquid sprays and crossflows.

250 to 130 K ft, a series of breakup tests were run in the Langley Mach 5.5 cyanogen-oxygen tunnel. This tunnel utilizes a stoichiometric cyanogen-oxygen combustion reaction, with a propellant flow rate of about 0.07 lb/sec to produce an 8-in. diam axisymmetric stream (with a 6-in. core) consisting of a mixture of two parts CO to 1 part N_2 at a stagnation pressure of one atmosphere and a stagnation temperature of 4500°K. This facility is unique in its ability to simulate typical values of the local gas dynamic parameters which are encountered along the afterbody of a blunt shape traveling at near orbital speeds. Parameters simulated and typical values for Mach 5.5 operation are: velocity (10,000 fps), static temperature (900°K), and static pressure

Table 1 Comparison of experimental jet break-up data

Ref.	Injectant	Gas stream	D_o, in.	Ambient press. torr.	T_i, °F	M	Re	Kn	We
				(a) Data from references					
2	Water	Argon	0.0165	6.5	70	3	8.56×10^2	5.68×10^{-3}	33.9
3	Water	Air	0.016	988	70	0.18	2.2×10^3	1.22×10^{-4}	21.9
3	Water	Air	0.040	988	70	0.18	5.6×10^3	4.9×10^{-5}	54.7
4	Water	Air	0.018	950	70	0.16	2.03×10^3	1.15×10^{-4}	14.2
8	Water	Air	0.020	2.8	80	8	9.60×10^2	1.23×10^{-2}	28.6
9	Water	Nitrogen	0.065	1794	70	0.06	5.66×10^3	1.52×10^{-5}	14.0
10	Water	Air	0.0145	82.8	70	2.8	1.0×10^3	4.15×10^{-5}	200
11	Iso-octane	Air	0.010	744	86	0.09	9.57×10^2	1.35×10^{-4}	27.6
11	Iso-octane	Air	0.020	744	86	0.09	1.18×10^3	1.09×10^{-4}	21.4
12	Water	Air	0.0135	823	73	0.66	5.58×10^3	1.75×10^{-4}	162
13	Water	Air	0.009	14.8	70	10.6	1.22×10^2	1.29×10^{-1}	31.5
14	Water	Air	0.020	744	76	0.09	1.14×10^3	1.15×10^{-4}	5.65
14	Water	Air	0.020	744	140	0.10	3.9×10^2	3.8×10^{-4}	6.23
14	Iso-octane	Air	0.020	744	88	0.09	9.6×10^2	1.14×10^{-4}	27.5
				(b) Present experiment					
Run 1	Water	2-CO, 1-N_2	0.010	0.48–0.36	44	5.45–5.67	5.2–4.7	1.48–1.89	3.9 to 3.2
Run 2	Water	2-CO, 1-N_2	0.021	0.36	46	5.45–5.67	11.0–8.9	0.70–0.90	8.3 to 6.7
Run 3	Water	2-CO, 1-N_2	0.040	0.36	42	5.45–5.67	21–17	0.37–0.47	15.7 to 12.8
Run 4	Water	2-CO, 1-N_2	0.080	0.36	40	5.45–5.67	42–34	0.19–0.24	31.4 to 25.7
				c) Typical flight (re-entry) values, RAM-C injection site at 233,000 ft					
	Water	Air	0.018	0.04	70	2.64	3.55	1.117	5.64

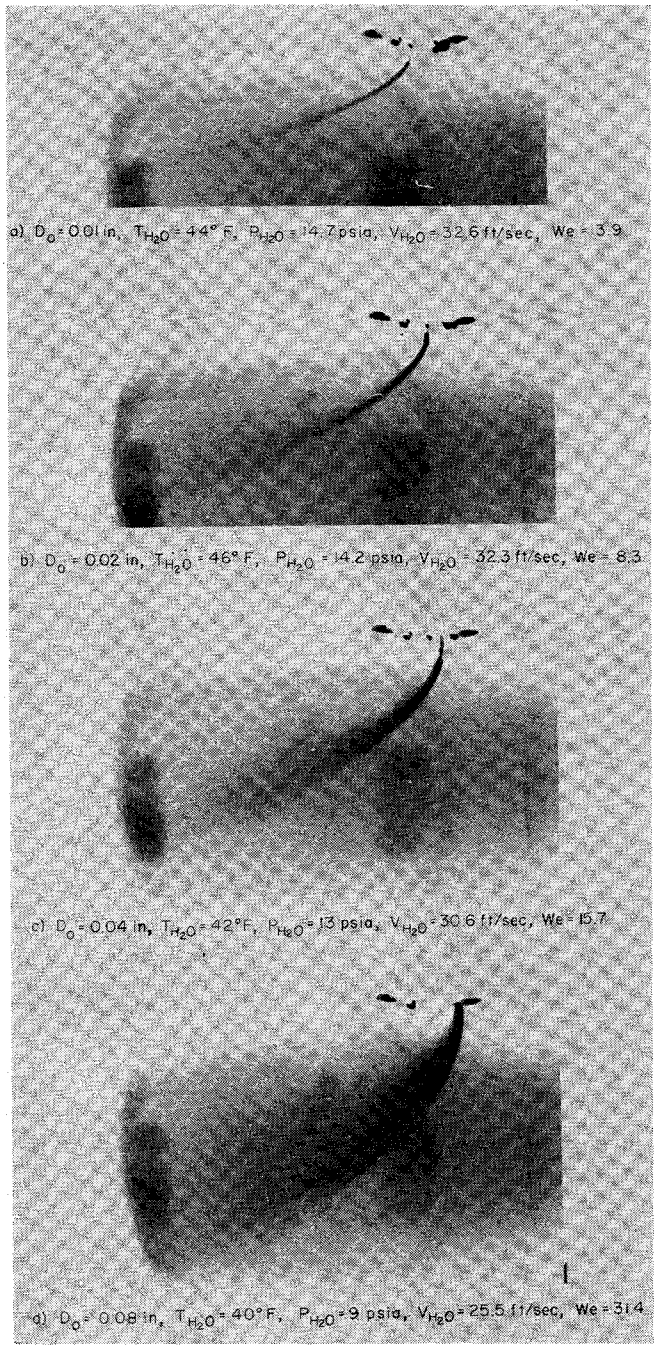

Fig. 2 Photographs of spray in M = 5.5, N_2 + 2 CO flow; T_t = 4500°K, T_{amb} = 825°K, P_{amb} = 0.48 Torr.

(1 lb/ft²). Of particular interest to the consideration of the problem of water ejected from blunt vehicles reentering at high altitudes is the question of possible effects of the locally high static temperatures upon breakup.[2] In the present facility it is possible to investigate the combined effect on jet breakup of both a low dynamic pressure and a high static temperature.

Since this tunnel has a conical nozzle, it produces a varying Mach number (5.45 to 5.67) and static density (1.6 to 1.3 × 10^{-5} lb ft^{-3}) over the region in which the spray is observed. The relative surface roughness of the spray orifices (ϵ/D_o) as estimated by microscopic examination was $\leq$0.01, and the length to diameter ratio was three. To be certain that vapor pressure breakup effects were of secondary importance, the spray water was injected cold at 40–46°F. The liquid delivery system consisted of an ice bath under atmospheric pressure, connected to the spray orifices through jacketed supply lines, control valves, and filter, to the jacketed spray manifold. Refrigerant at 35°F was circulated through the jackets and through coils in the ice bath and thence returned to a water cooler. To verify that the spray water was cold enough and therefore that aerodynamic breakup was the principal mechanism tending to atomize the jets, the test section was evacuated to 0.2 Torr and the jets operated without gas flow at the spray temperatures used for the runs with gas flow. All four jets formed transparent cylindrical streams which remained intact until striking the bottom of the test section. It was found necessary to heat the ends of the spray nozzles to prevent the spray water from freezing to the outside of the orifices and interfering with the jets. The temperature of the injected liquid was monitored by means of thermocouples located in the spray water immediately upstream of the spray orifices. It had been previously determined that the short residence time in the heated nozzle was not sufficient to warm the spray water appreciably.

The principal data were 16 mm ciné-camera photographs of the spray. Illumination was furnished by light from the combustion process passing out through the throat of the wind tunnel. Figure 2 is a reproduction of four frames of the 16 mm film showing successively, the spray from the 0.01, 0.02, 0.04, and 0.08-in.-diam orifices. The indistinct appearance of the lower portion of the jet from the 0.01-in.-diam orifice is believed due to small fluctuations in the position of the liquid stream during the exposure of the film. Direct visual observation gave the impression of complete coherence of the first inch or so of stream length. As expected, all four jets were bent or deflected downstream and the breakup process was found to be a function of jet diameter. The velocity of the liquid jets varied slightly from 32.6 fps for the 0.01-in.-diam orifice (Fig. 2a) with the least penetration, to 25.5 fps for the 0.08-in.-diam orifice with the most penetration. The data for the jets of the present experiment are tabulated in Table 1b and plotted as squares in Fig. 1. The critical orifice diameter is seen to be approximately 0.02 in., and the $We_{crit} \approx 6$ for the Knudsen numbers in these tests, which were of order 1.0.

It should be noted that the data of Fig. 1 are insufficient to describe with certainty the variation of critical Weber number between continuum and free molecular flow. However, recent unpublished wind-tunnel data taken at M = 4.6, We = 7.5 and $Kn = 2 \times 10^{-2}$ in air, while not extending into the no-breakup regime, indicate that the boundary is indeed a straight line and that there is no effect of Knudsen number or high local static temperature on critical Weber number for primary atomization of liquid jets injected into a gaseous crossflow.

References

[1] Evans, J. S., "Reduction of Free Electron Concentration in a Reentry Plasma by Injection of Liquids," *Proceedings of the Third Symposium on the Plasma Sheath*, Vol. III, May 1967, Air Force Cambridge Research Labs., pp. 343–355.

[2] Kurzius, S. C. and Raab, F. H., "Measurement of Droplet Sizes in Liquid Jets Atomized in Low Density Supersonic Streams," CR-1242, Dec. 1968, NASA.

[3] Priem, R. J., "Breakup of Water Drops and Sprays with a Shock Wave," *Jet Propulsion*, Vol. 27, No. 10, 1957, pp. 1084–1087.

[4] Morrell, G., "Rate of Liquid Jet Breakup by a Transverse Shock Wave," TN D-1728, May 1963, NASA.

[5] Rayleigh, L., "On the Instability of Jets," *Proceedings of the London Mathematical Society*, Vol. 10, 1879, pp. 4–13.

[6] Luna, R. E. and Klikoff, W. A., Jr., "Aerodynamic Breakup of Liquid Drops," Rept. SC-RR-66-2716, June 1967, Scandia Corp., Albuquerque, N. Mex.

[7] Bushnell, D. M. and Gooderum, P. B., "Atomization of Superheated Water Jets at Low Ambient Pressures," *Journal of Spacecraft and Rockets*, Vol. 5, No. 2, Feb. 1968, pp. 231–232.

[8] Gooderum, P. B., Bushnell, D., and Huffman, J., "Mean Droplet Size for Cross-Stream Water Injection into a Mach 8 Air Flow," *Journal of Spacecraft and Rockets*, Vol. 4, No. 4, April 1967, pp. 534–536.

[9] Clark, B. J., "Breakup of a Liquid Jet in a Transverse Flow of Gas," TN D-2424, Aug. 1964, NASA.
[10] Kolpin, M. A., Horn, K. P., and Reichenback, R. E., "Study of Penetration of a Liquid Injectant into a Supersonic Flow," *AIAA Journal*, Vol. 6, No. 5, May 1968, pp. 853–858.
[11] Ingebo, R. D., "Penetration of Drops into High-Velocity Airstreams," TM X-1363, April 1967, NASA.
[12] Chelko, L. J., "Penetration of Liquid Jets into a High-Velocity Air Stream," RM E50F21, Aug. 1950, NACA.
[13] Weaver, W. L. and Hinson, W. F., "Water Injection from a 9° Hemisphere-Cone into a Hypersonic Airstream," TND-5739, March 1970, NASA.
[14] Ingebo, R. D. and Foster, H. H., "Drop-Size Distribution for Cross-current Breakup of Liquid Jets in Airstreams," TN 4087, Oct. 1957, NACA.
[15] Morrell, G., "Critical Conditions for Drop and Jet Shattering," TN D-677, Feb. 1961, NASA.
[16] Haas, F. C., "Stability of Droplets Suddenly Exposed to a High Velocity Gas Stream," *AIChE Journal*, Vol. 10, No. 6, Nov. 1964, pp. 920–924.
[17] Evans, J. S., Schexnayder, C. J., and Huber, P. W., "Computation of Ionization in Reentry Flow Fields," *AIAA Journal*, Vol. 8, No. 6, June 1970, pp. 1082–1089.

Effect of a Spike on the Drag and on the Aerodynamic Stability of Blunt Bodies in Supersonic Flow

CARLOS ZOREA* AND JOSEF ROM†
Technion—Israel Institute of Technology, Haifa, Israel

Nomenclature

a	=	spike's diameter (= $d/16$ in present study)
C_D, C_L	=	drag and lift coefficients D/qS and L/qS
C_m	=	moment coefficient $\bar{M}/q\,Sd$
d	=	body diameter (= hemispherical nose diameter)
D, L	=	drag and lift forces, respectively
l	=	spike length
M_∞	=	Mach number of undisturbed freestream
$\bar{M}$	=	pitching moment
$p, \Delta p$	=	pressure and pressure rise respectively
q	=	dynamic pressure, $\rho V^2/2$
Re_d	=	Reynolds number based on diameter
Re_f	=	Reynolds number based on the length from the spike's tip apex to the tip shoulder
S	=	reference area
V	=	velocity
$x_{a.c.}$	=	position of the aerodynamic center (measured from the base)
α	=	angle of attack
θ_c	=	equivalent cone half-angle of the separated flow on the spike
ρ	=	air density

Subscripts

b, F, n	=	base, forebody, and nose, respectively
crit	=	critical
max	=	maximum

Introduction

SPIKES have been used to reduce the wave drag of a blunt nose by converting the flow from a blunt-body pattern to an essentially conical flow pattern.[1–12] The spike establishes a conical separated flow zone when it is of a proper length. When a certain critical spike length is exceeded, the separation moves from the spike tip to some position on its length, and the effectiveness of the spike is greatly reduced. A method for estimating this critical spike length is presented in this Note. Some studies[5,8–10] have shown that the effect of the spike on the nose drag is diminished as the angle of attack α increases. The effect of the spike on the static stability is very small.[11] In the present investigation these effects are studied at Mach numbers 1.5 and 2.25 at various Reynolds numbers and spike lengths. The results provide a better understanding of these effects.

Received March 4, 1970; revision received April 21, 1970. This paper is based in parts on the thesis presented by C. Zorea to the Senate of the Technion, Israel Institute of Technology in partial fulfilment of the requirements for the M.Sc. degree.

* Graduate Student and Research Engineer, Scientific Department, Ministry of Defence, Government of Israel.
† Professor, Department of Aeronautical Engineering. Associate Fellow AIAA.

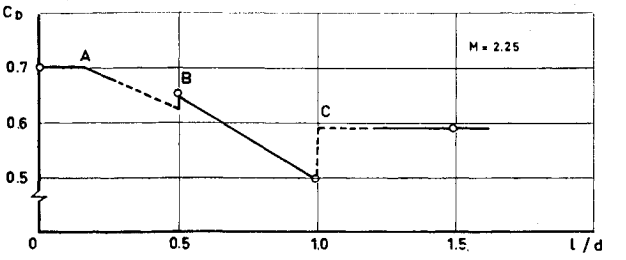

Fig. 1 Variation of the forebody drag coefficient with spike length.

The experiments were done in the 30 cm × 30 cm supersonic blow down wind tunnel at the Aerodynamic Laboratory of the Department of Aeronautical Engineering. The models are cylindrical bodies 28 mm in diameter by 180 mm long, hemispheric and ogive with a hemispherical nose of 11 mm radius. The spike is installed in the nose center. Its diameter (a = 1.75 mm) is $\frac{1}{16}$ of the model's body diameter (d = 28 mm) and its tip is conical with half-angle of 10°. The spike length l is varied to give l/d values of 0, 0.5, 1.0, 1.5, and 2.0. The aerodynamic forces and moments are measured by a 3-component, strain-gage balance. The flow is photographed by a Schlieren or a shadow optical system using movie photography (24 to 80 frames/sec) and by a Polaroid camera.

Critical Spike Length

At low supersonic Mach numbers (i.e. $M_\infty < 1.5$) the conical wave drag coefficient is higher than the corresponding blunt-body wave drag coefficient. At higher M_∞, the blunt-body drag becomes the much larger, and the drag coefficient varies with spike length as shown in Fig. 1 for M_∞ = 2.25. (The circles represent measured values.) The initial drag level, extending up to Point A, corresponds to the conditions where the spike is shorter than the detached shock-wave stand-off distance for the blunt nose. As the spike length is increased further, from A to B and to C, the over-all wave drag is reduced as the conical flow becomes shallower. A small local increase in drag is expected at point B where the separation shock moves from the spike's tip to the tip shoulder as shown

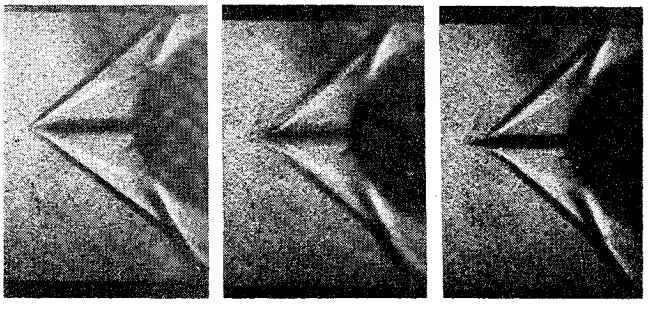

Fig. 2 Shadowgraph of the flow on the model with a spike. M = 2.25, l/d = 0.5, $Re_f = 2 \times 10^5$.